Journal of Radioanalytical and Nuclear Chemistry (2021) 329:1001–1009
https://doi.org/10.1007/s10967-021-07806-9

# Adsorption and separation behavior of strontium and yttrium using a silica-based bis(2-ethylhexyl) hydrogen phosphate adsorbent

**Taiga Kawamura**[1,2] · **Hao Wu**[1] · **Seong-Yun Kim**[1]

Received: 12 April 2021 / Accepted: 24 May 2021 / Published online: 5 June 2021

## Abstract

(HDEHP + Hexa)/$SiO_2$-P, a silica-based adsorbent, was prepared and used to separate Y(III) from a mixed solution of Sr(II) and Y(III). The adsorption behavior of the adsorbent was investigated using batch tests. The adsorbent exhibited high adsorption performance for Y(III) in low nitric acid concentrations and weak adsorption performance for Y(III) at higher concentrations. In contrast, Sr(II) was not adsorbed in either acid concentration range. The same tendency was observed under hydrochloric acid conditions. Y(III) separation from a mixed solution of Sr(II) and Y(III) was verified by a column test. Overall, the (HDEHP + Hexa)/$SiO_2$-P adsorbent can separate Y(III) from Sr(II).

**Keywords** HDEHP-impregnated adsorbent · Strontium · Yttrium · Separation · Extraction chromatography

## Introduction

High-level liquid waste (HLLW) generated by spent nuclear fuel reprocessing includes large quantities of Sr and Y isotopes (~1.1 kg/1 tHU, 45 GWd/t) [1, 2]. $^{90}$Sr and $^{90}$Y are the main isotopes of Sr and Y that generate considerable heat in HLLW. $^{90}$Sr decays to $^{90}$Y by emitting a β-ray with a half-life of approximately 28 years.

$^{90}$Y is a radioisotope used as a radiopharmaceutical in nuclear medicine for various therapeutic applications, for example therapeutic agent for Malignant lymphoma. As $^{90}$Y is present in mixed solutions of $^{90}$Sr and $^{90}$Y, it is vital to separate $^{90}$Y from the solution to be used as a radiopharmaceutical [3, 4]. $^{90}$Y is the major daughter nuclide in the $^{90}$Sr decay system and emits 2.28 MeV β-rays due to radioactive decay with a half-life of approximately 64 h to become a stable daughter nuclide, $^{90}$Zr. This is represented by the following reaction:

$$^{90}Sr \xrightarrow[\beta^-(0.54\mathrm{MeV},28.8\mathrm{y})]{} {}^{90}Y \xrightarrow[\beta^-(2.28\mathrm{MeV},64h)]{} {}^{90}Zr(stable) \tag{1}$$

Therefore, the selective separation of $^{90}$Sr and $^{90}$Y from HLLW is essential from the point of view of nuclear waste management.

Yttrium is a rare earth metal used in various applications such as radiation therapy and materials for industrial products. Nevertheless, to use it, it is essential to separate yttrium from mixtures with other metals. In recent years, various methods for separating yttrium from metals mixture have been studied. The separation of yttrium by a precipitation method was reported. In this study, a method of separating yttrium from a CRT (cathode ray tube) was reported to reduce waste and recover and reuse valuable metals from the viewpoint of environmental protection. In this method, the CRT was dissolved in sulfuric acid, and the yttrium in the resulting solution was recovered by precipitation with $C_2H_4O_2$ (Valentina et al.) [5]. A solvent extraction method and an ion exchange method to extract yttrium from a mixed solution of rare earth elements have been evaluated. An extraction system using sec-octylphenoxy acetic acid (CA12) and bis (2,4,4-trimethylpentyl) phosphinic acid (Cyanex272) achieved the high-purity separation of yttrium from rare earth ores using a solvent extraction method (Yanliang et al.) [6]. In addition, yttrium was separated selectively from a mixed solution of rare earth elements using an ion-exchange method on a C18 column with tetra-n-butylammonium hydroxide (TBAOH) as the ion interaction

---

✉ Seong-Yun Kim
sonyun.kimu.d7@tohoku.ac.jp

[1] Department of Quantum Science and Energy Engineering, Graduate School of Engineering, Tohoku University, 6-6-01-2 Aza-Aoba-Aramaki, Aoba-ku, Sendai, Miyagi 980-8579, Japan

[2] Japan Nuclear Fuel Limited, 4-108 Aza-Okitsuke, Oaza Obuchi, Rokkasyo-mura, Kamikita-gun, Aomori 039-3212, Japan

reagent and nitrilotriacetic acid (NTA) as the complexing agent (Rajmunds et al.) [7]. The separation of yttrium using ionic liquids has also been reported; bifunctional ionic liquids [CA12] [methyltrioctyl ammonium (N1888)] could separate yttrium from rare earth concentrates (Yanliang et al.) [8]. Research on extraction chromatography using an adsorbent with an organic extractant immobilized on a solid phase was also conducted. The daughter nuclide, $^{90}$Y, was separated from seawater using diglycolamide (DGA) resin and measured to monitor the $^{90}$Sr released into the ocean due to the incident at the Fukushima Daiichi Nuclear Power Plant (Tazoe et al.) [9].

A microporous silica/polymer composite carrier ($SiO_2$-P) has been used to fix the organic extractant. $SiO_2$-P is an inorganic/organic hybrid material prepared by impregnating a macroporous $SiO_2$ substrate with a copolymer. $SiO_2$-P is a promising carrier for extractants due to its strong acidity, mechanical strength, radiation resistance, and easy separation of solids and liquids. Research on separation using adsorbents with various extractants impregnated into $SiO_2$-P has also been conducted. Y can be separated from a mixed solution of Sr(II) and Y(III) using a *N*,*N*,*N*′,*N*′-tetra-*n*-octyl-diglycolamide (TODGA) impregnated adsorbent (Xu et al.), a 4’4’(5’)-di(tert-butylcyclohexano)-18-crown-6 (DtBuCH18C6) impregnated adsorbent (Kim et al.) or an octyl(phenyl)-*N*,*N*-diisobutylcarbamoyl methylphosphine oxide (CMPO) impregnated adsorbent (Kawamura et al.) [10–12].

In this study, bis-(2-ethylhexyl) phosphoric acid (HDEHP) was used as an extractant; Fig. 1 shows its molecular structure. HDEHP is a trivalent cation extractor. Because Y(III) exists as a trivalent cation in solution, Y(III) might be separated from a mixed solution of Sr(II) and Y(III) using HDEHP. The above research is summarized in Table 1.

The silica-based HDEHP adsorbent was prepared by impregnating HDEHP and 1-hexanol as a molecule modifier into $SiO_2$-P. The effects of the acid concentration, contact time, temperature, and metal ion concentration for the adsorbent were investigated to understand Y(III) adsorption and separation. Y(III) was separated from a mixed solution of Sr(II) and Y(III) with HDEHP adsorbent using a column test.

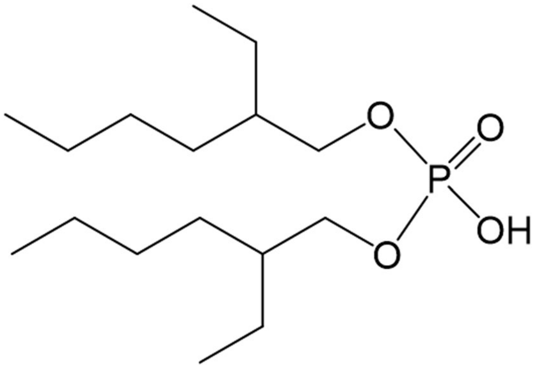

**Fig. 1** Molecular structure of HDEHP

**Table 1** Summary of recent research

| Method | Result | Recovery of Y | References |
|---|---|---|---|
| Precipitation | Yttrium was precipitated using $C_2H_4O_2$ from the solution dissolved CRT | 75–80% of the total | Valentina et al. [5] |
| Solvent extraction | Yttrium was separated from rare earth ores using CA12 and Cyanex272 | 95% of the total | Yanliang et al. [6] |
| Ion-exchange | Yttrium was separated from the mixed solution of rare earth using TBAOH and NTA | Completely separated | Rajmunds et al. [7] |
| Ionic liquid | Yttrium was separated from the rare earth solution using the ionic liquid of [CA12][N1888)] | Purity of 98.5 wt% | Yanliang et al. [8] |
| Extraction chromatography | Yttrium was separated from the mixed solution of Strontium and Yttrium using the DGA-resin | 95.5% of the total | Tazoe et al. [9] |
| Extraction chromatography | Yttrium was separated from the mixed solution of Strontium and Yttrium using the TODGA adsorbent | 100% of the total | Xu et al. [10] |
| Extraction chromatography | Yttrium was separated from the mixed solution of Strontium and Yttrium using the DtBuCH18C6 adsorbent<br>(Sr(II) was adsorbed on the adsorbent) | Completely separated (no adsorption) | Kim et al. [11] |
| Extraction chromatography | Yttrium was separated from the mixed solution of Strontium and Yttrium using the CMPO adsorbent | Almost 100% of the total | Kawamura et al. [12] |
| Extraction chromatography | This study (using HDEHP adsorbent) | | |

## Experimental

### Materials

HDEHP was obtained from Tokyo Chemical Industry Co., LTD. $Sr(NO_3)_2$ (98%) and $SrCl_2$ (95%) were obtained from Wako Pure Chemical Industries, Ltd. $Y(NO_3)_3 \cdot 6H_2O$ (99.99%) and $YCl_3 \cdot 6H_2O$ (99.99%) were supplied by Kanto Chemical Co.

### Preparation of adsorbent

In this study, the adsorbent was prepared by impregnating the HDEHP extractant into $SiO_2$-P and 1-hexanol (Hexa) as a molecule modifier into $SiO_2$-P. The $SiO_2$-P particles were washed three times with approximately 300 $cm^3$ of methanol and vacuum dried for 1 day. The extractant HDEHP was dissolved in approximately 200 $cm^3$ dichloromethane, used as a diluent, with a molecule modifier 1-hexanol. $SiO_2$-P was mixed with dichloromethane. After the mixture was stirred for approximately 1.5 h, the dichloromethane was removed using a rotary evaporator. The residue was vacuum dried at 313 K for one day and the adsorbent (HDEHP+Hexa)/$SiO_2$-P was obtained [12].

### Batch method

The Sr(II) and Y(III) adsorption behaviors onto (HDEHP+Hexa)/$SiO_2$-P were examined using a batch method. Approximately 0.2 g of the dry adsorbent was divided into 13.5 $cm^3$ glass vials, and 4 $cm^3$ of the liquid solution was added to the glass vials. The glass vials were shaken at 160 rpm for 10 min to 5 h in a thermostatic shaking bath. The solution was either $HNO_3$ or HCl containing different concentrations of Sr (II) and Y (III), each having different acid concentrations. [12]

The adsorbents and the solution were separated by filtration after shaking. The concentrations of the metal ions in the solution were measured by inductively coupled plasma-atomic emission spectrometry (ICP-AES, Shimadzu ICPE-9000). The distribution coefficients ($K_d$, $cm^3/g$) and uptake ratios ($R$, %) of the Sr(II) and Y(III) ions were calculated as follows:

$$K_d = \frac{C_0 - C_e}{C_e} \times \frac{V}{m} \tag{2}$$

$$R = \frac{C_0 - C_e}{C_0} \times 100 \tag{3}$$

where $C_0$ and $C_e$ are the concentrations of metal ion before and after adsorption in the solution in ppm, respectively; $m$ is the dry adsorbent weight in g, and $V$ is the solution volume in $cm^3$.

### Column method

Approximately 3 g of (HDEHP+Hexa)/$SiO_2$-P adsorbent and water were placed in a glass beaker, and the adsorbent was degassed by suction. Subsequently, the adsorbent was packed into a glass column (8 mm inner diameter × 100 mm length) and prepared.

The column test was conducted under two conditions: nitric acid and hydrochloric acid. Several solutions were passed through the column using a metering pump. The temperature of the column was maintained at 298 K using a thermostatic water jacket, and the flow rate during the column test was approximately 0.5 $cm^3$/min.

Under the nitric acid condition, 0.5 M $HNO_3$ solutions containing 10 mM Sr(II) and Y(III) were fed into the column as the feed solutions. A 0.5 M $HNO_3$ solution containing no metal ions was fed continuously into the column as a washing solution. 3 M $HNO_3$ was also fed into the column after 0.5 M $HNO_3$ to elute the metal ions adsorbed on the adsorbent. As the solutions were fed to the column, the solution out from the column was collected in 5 ml tubes using a fraction collector. ICP-AES measured the Sr(II) and Y(III) concentrations in each tube. Under the hydrochloric acid conditions, the experiment was carried out in the same procedure [12].

## Results and discussion

### Effect of the acid concentration

A batch test was conducted to understand the effects of the acid concentration on the adsorption behavior [10–15]. Figure 2 shows the effects of the acid concentration on the (HDEHP+Hexa)/$SiO_2$-P adsorbent. Under nitric acid conditions, the (HDEHP+Hexa)/$SiO_2$-P adsorbent showed high adsorption affinity for Y(III) in the range of low acid concentrations (0.001–0.1 M). At higher acid concentrations, the adsorption affinity decreased with increasing acid concentration, and the uptake ratio was a few percent from 3 to 5 M $HNO_3$. On the other hand, Sr(II) was barely adsorbed onto the adsorbent at any acid concentration.

Under the HCl condition, the tendency of adsorption was similar to the case of the $HNO_3$ condition. Sr(II) was barely adsorbed onto the adsorbent at any acid concentration. Y(III) was well adsorbed onto the (HDEHP+Hexa)/$SiO_2$-P adsorbent at low acid concentrations, and the ratio decreased at higher acid concentrations. On the other hand, the difference was

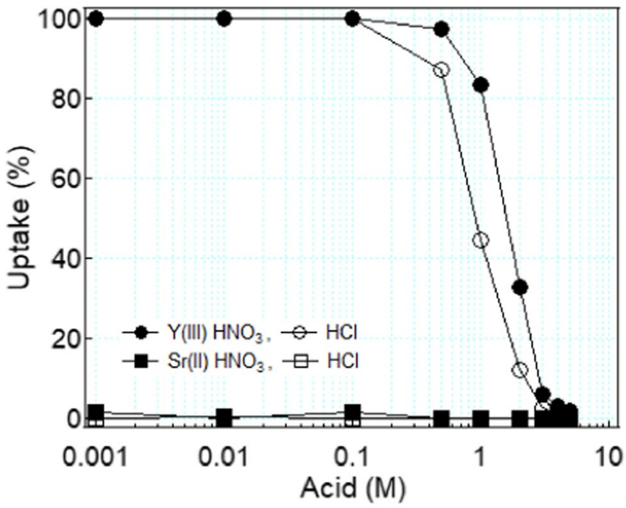

**Fig. 2** Effects of the acid concentration on (HDEHP + Hexa)/$SiO_2$-P adsorbent

large at a 1 M acid concentration. The uptake ratio under the $HNO_3$ condition was more than 80%, whereas it was less than 50% under the HCl condition. Therefore, (HDEHP+Hexa)/$SiO_2$-P adsorbent showed good selectivity for the adsorption of Y(III) at low acid concentration.

Peppard proposed the extraction of trivalent lanthanides by HDEHP and reported that the metal ($M^{3+}$) is coordinated to three HDEHP dimers $(HDEHP)_2$. [16] The mechanism can be represented by eq. (4):

$$Y^{3+} + 3(HDEHP)_2 \rightleftarrows Y(H(DEHP)_2)_3 + 3H^+ \tag{4}$$

As the $H^+$ concentration in the solution increases, the chemical equilibrium shifts to the left, and $Y(H(DEHP)_2)_3$ decreases, according to Eqs. (4). This suggests that the adsorption weakens as the acid concentration increases, regardless of the type of acid.

These results suggest that it is possible to separate Y(III) and Sr(II) with a low acid concentration (<0.5 M) and elute Y(III) with a high acid concentration (>3 M).

## Effect of contact time

A batch test was conducted to understand the effects of the contact time on the adsorption behavior. The kinetic data of the adsorption was fitted to a pseudo-second-order equation:

$$Q_t = \frac{k_2 Q_e^2 t}{1 + k_2 Q_e t}(\text{non-linear}) \tag{5}$$

$$\frac{t}{Q_t} = \frac{1}{k_2 Q_e^2} + \frac{t}{Q_e}(\text{linear}) \tag{6}$$

where $Q_t$ and $Q_e$ are the amounts of Y(III) adsorbed at time $t$ and equilibrium (mg/g), respectively; $k_2$ is the rate constant of the pseudo-second-order adsorption (g/mg h). These models are commonly used to describe adsorption behavior. In this model, the adsorption process seemed to be chemical adsorption, and the adsorption capacity is proportional to the number of active sites. [17–20]

Figure 3 shows plots of $t/Q_t$ versus time. Figure 4 shows plots of $Q_t$ versus time fitted to the pseudo-second-order kinetic model. In Fig.3, plots of $t/Q_t$ versus time showed a straight line, and the correlation coefficient ($R^2$) was approximately 1.00. This indicates that the adsorption process was fitted well to the pseudo-second-order model.

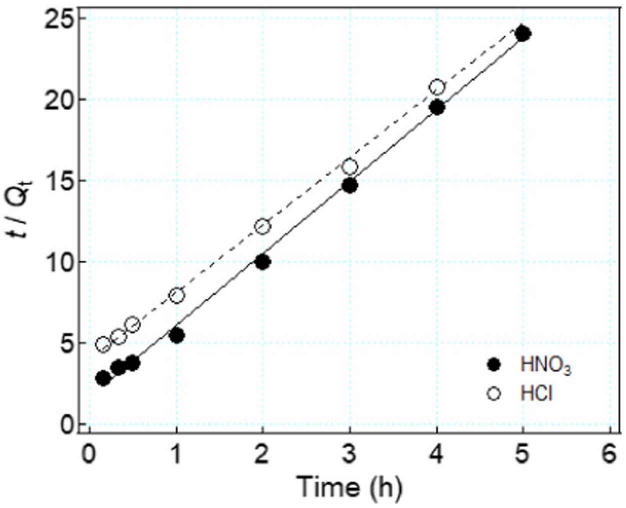

**Fig. 3** Pseudo-second-order kinetic fit for Y(III) adsorption onto the (HDEHP + Hexa)/$SiO_2$-P adsorbent. (linear)

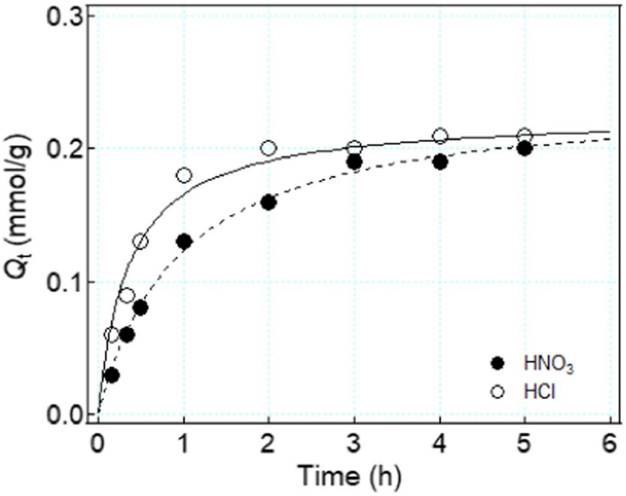

**Fig. 4** Pseudo-second-order kinetic fit for Y(III) adsorption onto the (HDEHP + Hexa)/$SiO_2$-P adsorbent. (non-linear)

**Table 2** Pseudo-second-order kinetic model parameter

| Parameters | $HNO_3$ | HCl |
|---|---|---|
| $k_2$ | 12.3 | 4.38 |
| $Q_e$ (mmol/g) | 0.23 | 0.24 |
| $R^2$ | 1.00 | 1.00 |

$Q_e$ and $k$ were calculated from the slope of the straight line and are summarized in Table 2. The $Q_e$ value was determined to be 0.23 mmol/g and 0.24 mmol/g under the $HNO_3$ and HCl conditions, respectively. Although the experimental value was lower than the calculated $Q_e$, a value close to the calculated value can be obtained by continuing until the reaction reaches equilibrium.

## Effects of temperature

A batch test was conducted at 288 K, 298 K, and 308 K under the $HNO_3$ and HCl conditions to understand the effects of temperature on the adsorption behavior. The thermodynamic properties of adsorption of Y(III) to (HDEHP+Hexa)/$SiO_2$-P were investigated by calculating some thermodynamic parameters using from these results Van't Hoff's equation [21–23].

The Van't Hoff equation is expressed as

$$\Delta G^o = \Delta H^o - T\Delta S^o \quad (7)$$

$$lnK_d = \frac{\Delta S^0}{R} - \frac{\Delta H^0}{RT} \quad (8)$$

where $\Delta G^0$ is the change in Gibbs free energy (kJ/mol), $\Delta H^0$ is the change in standard enthalpy (kJ/mol) and $\Delta S^0$ is the change in standard entropy (J/K·mol). $T$ is the temperature (K), and $R$ is the gas constant (8.314 J/mol·K); $K_d$ is the same as Eq. (2).

Figure 5 shows plots of ln($K_d$) versus $1/T$. Both relationships were linear, and the correlation coefficient ($R^2$) was approximately one. The $ln(K_d)$ value increased as $1/T$ was increased, and the slope was larger under the $HNO_3$ condition than under the HCl condition. $\Delta H^0$ and $\Delta S^0$ were determined from the slope and intercept of the plots of $ln(K_d)$ vs. $1/T$. The values of $\Delta H^0$ and $\Delta S^0$ were negative under both solution conditions. The adsorption processes of Y(III) on (HDEHP+Hexa)/$SiO_2$-P adsorbent were exothermic. $\Delta G^0$ was calculated for each temperature and summarized in Table 3. The values of $\Delta G^0$ for each temperature were negative and decreased with increasing temperature. Hence, the adsorption reaction progresses spontaneously, and it readily adsorbs at high temperatures.

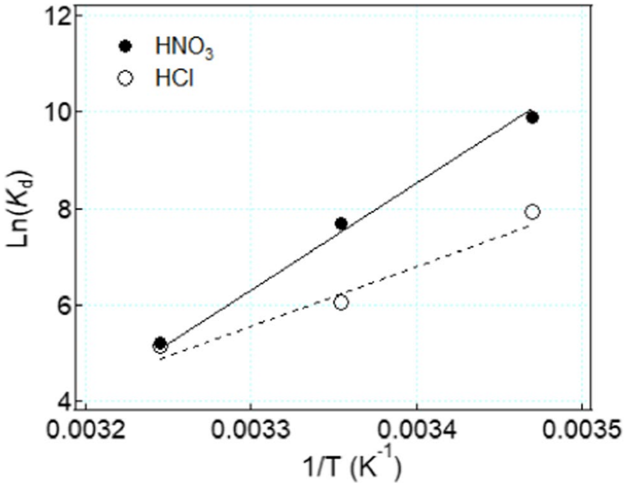

**Fig. 5** Effects of temperature on the (HDEHP + Hexa)/$SiO_2$-P adsorbent

## Adsorption isotherm

The adsorption mechanism was assessed by conducting a batch test in $HNO_3$ and HCl solutions with various metal concentrations and compared using three adsorption models: Langmuir equation, Freundlich equation, and Dubinin–Raddushkevitch (D–R) equation. [24–26] The adsorption isotherm shows the relationship between the adsorbate concentration at equilibrium and the amount of adsorbate on the adsorbent.

The Langmuir equation represents adsorption, assuming that the adsorption sites are distributed uniformly and are monolayered. The Dubinin–Raddushkevitch equation assumes that the adsorption sites are non-uniform. The Freundlich equation is an empirical formula for adsorption equilibrium; it is usually applied to multi-layer and non-uniform surface adsorption.

The Langmuir equation, Freundlich equation and Dubinin–Raddushkevitch equation are given by the following:

**Table 3** Thermodynamic parameters for the Y(III) adsorption on (HDEHP+Hexa)/$SiO_2$-P adsorbent

| | $HNO_3$ | HCl |
|---|---|---|
| $\Delta S$ (kJ/K/mol) | −5.52E−01 | −2.93E−01 |
| $\Delta H$ (kJ/mol) | −1.83E+02 | −1.03E+02 |
| $\Delta G$ (kJ/mol) | | |
| 288.15 (K) | −2.41E+01 | −1.83E+01 |
| 298.15 (K) | −1.86E+01 | −1.54E+01 |
| 308.15 (K) | −1.31E+01 | −1.25E+01 |

$$\text{Langmuir equation: } Q_{\text{eq}} = \frac{q_m K_L C_{\text{eq}}}{1 + K_L C_{\text{eq}}} \tag{9}$$

$$\text{Freundlich equation: } Q_{\text{eq}} = K_f C_{\text{eq}}^{\frac{1}{n}} \tag{10}$$

$$\text{Dubinin−Radushkevich equation: } Q_{\text{eq}} = q_m exp(-K_{ad}\varepsilon^2) \tag{11}$$

$$\varepsilon = RT\ln(1 + \frac{1}{C_e}) \tag{12}$$

where $C_{\text{eq}}$ (mol/L) and $Q_{\text{eq}}$ (mol/g) are the equilibrium concentration of Y(III) in the aqueous and solid phases, respectively. $q_m$ (mol/g) is the maximum capacity of Y(III) taken up. $K_L$ (L/mol), $K_f$ (mol/g), and $K_{ad}$ (mol$^2$/kJ$^2$) are the Langmuir constant, Freundlich constant, and Dubinin–Radushkevich constant, respectively. n is an exponential constant related to the adsorption strength of the Freundlich model. $R$ is the gas constant (8.314 J/mol K) and $T$ is the temperature (K).

Table 4 summarizes the values of each constant, the maximum capacity, and the correlation coefficients for Y(III) ions. Figure 6 shows a non-linear relationship in each model. A comparison of the parameters closely resembled the Langmuir model under both conditions, suggesting that both adsorption processes appear to be single-layer adsorption.

In the Langmuir model, the maximum adsorption capacity of Y(III) on the (HDEHP+Hexa)/SiO$_2$-P adsorbent was 0.26 mmol/g under HNO$_3$ conditions and 0.31 mmol/g under HCl conditions.

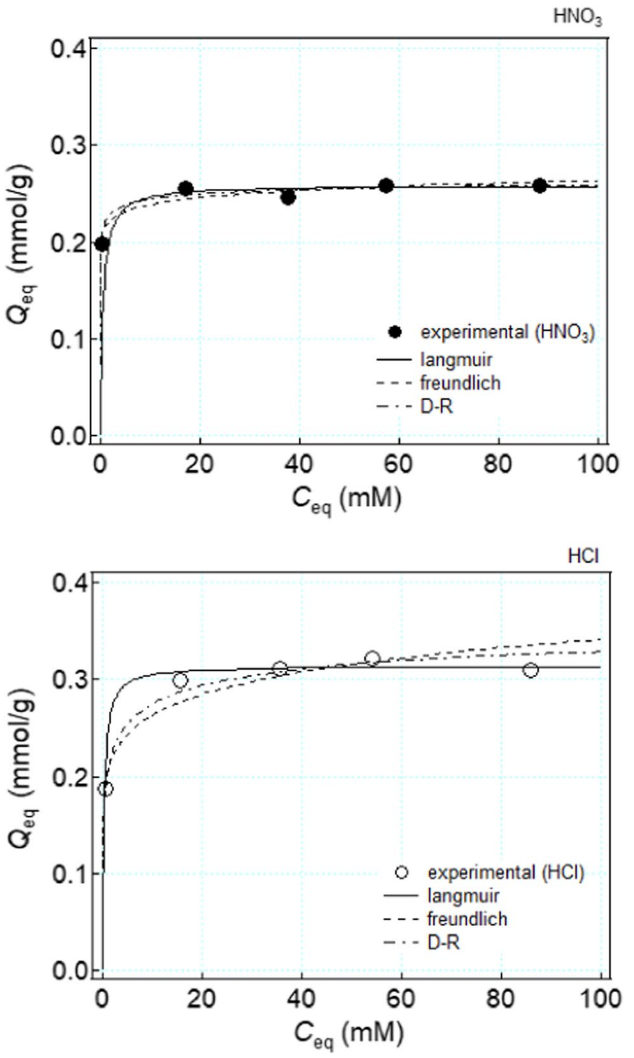

**Fig. 6** Adsorption isotherm of metal ions on (HDEHP + Hexa)/SiO$_2$-P adsorbent

**Table 4** Langmuir, Freundlich, and Dubinin–Radushkevich isotherm parameters constants

| Parameters | HNO$_3$ | HCl |
|---|---|---|
| Langmuir | | |
| $Q_{max}$ (mmol/g) | 0.26 | 0.31 |
| $K_L$ (l/mol) | 1.97 | 3.25 |
| $R^2$ | 1.00 | 1.00 |
| Freundlich | | |
| $K_F$ (mmol/g) | 0.22 | 0.20 |
| $1/n$ | 0.04 | 0.11 |
| $R^2$ | 0.94 | 0.93 |
| Dubinin–Radushkevich | | |
| $Q_{max}$ (mol/g) | 0.26 | 0.35 |
| $\varepsilon$ (mol$^2$/J$^2$) | 6.18E−10 | 1.9E−09 |
| $R^2$ | 0.96 | 0.98 |

## Column separation

A column test was conducted to determine if Y could be separated and recovered from a mixed solution of Sr(II) and Y(III). Figure 7 presents the extraction chromatography results of separating Y(III) from a mixed solution of Sr(II) and Y(III) using (HDEHP+Hexa)/SiO$_2$-P adsorbent in HNO$_3$ or HCl solutions. In a HNO$_3$ solution, Sr(II) was not adsorbed and immediately flowed out of the column. On the other hand, Y(III) was retained. Subsequently, when H$_2$O was supplied to the column, the Y(III) adsorbed on the adsorbent was eluted from the column. The behavior was similar under the HCl solution conditions to that under the HNO$_3$ conditions.

The elution rate of Y(III) from the column was different. A clear elution peak of Y(III) was observed when the

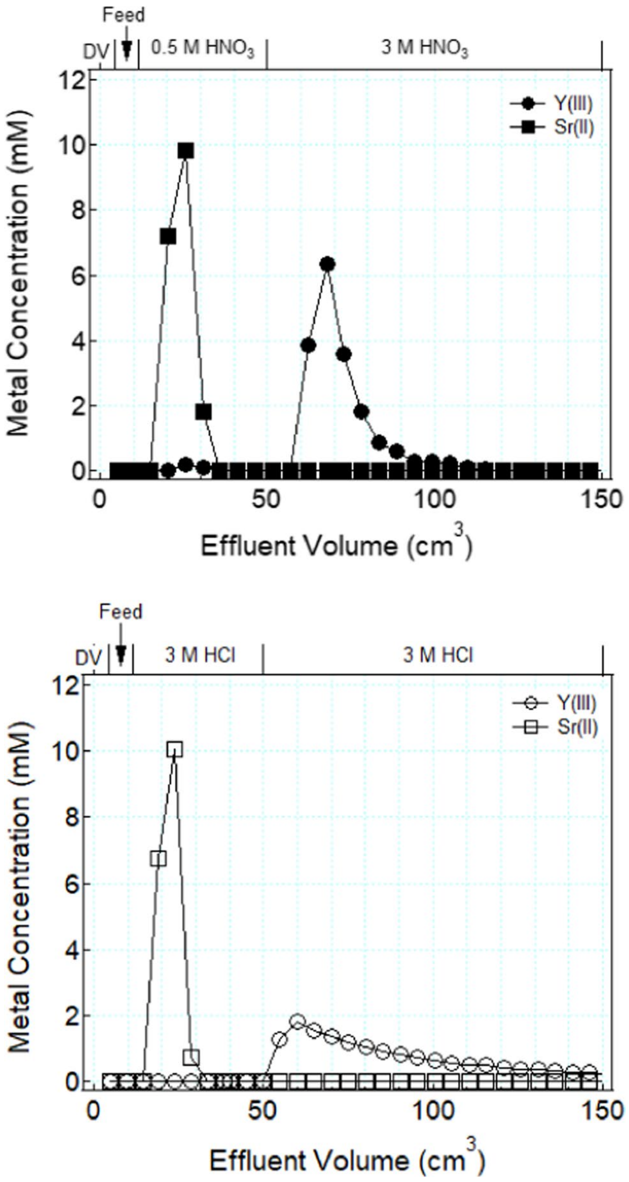

**Fig. 7** Column separation results for Sr(II) and Y(III) from $HNO_3$ and HCl solution using (HDEHP + Hexa)/$SiO_2$-P adsorbent

$HNO_3$ solution was used, but the elution of Y(III) was continuous when the HCl solution was used.

The chemical yield of Y(III) from the start of elution and end of elution was calculated to be approximately 90 wt% under the $HNO_3$ solution. The column test showed that it was possible to separate and recover Y(III) from a mixed solution of Sr(II) and Y(III) using the (HDEHP+Hexa)/$SiO_2$-P adsorbent.

Table 5 compares the present result with the results of separation using the TODGA, DtBuCH18C6, and CMPO adsorbents reported elsewhere. Although the recovery rate of the HDEHP adsorbent was slightly lower than that of the other adsorbents, a high recovery rate of 90% was still achieved. The HDEHP adsorbent showed considerably higher $K_d$ and $Q_e$ values than the other adsorbents in nitric acid. This is because the complex of yttrium with HDEHP has a stronger bond than with the other extractants. These results indicate that the amount of yttrium adsorbed onto the HDEHP adsorbent is more than the other adsorbents when the amount of adsorbent is the same.

In addition, the $k_2$ value was the second-fastest after the 1-dodecanol-added CMPO adsorbent, confirming that the adsorption rate was sufficiently high. Therefore, there is no need to slow down the flow rate of the feed solution to the column or lengthen the column.

This suggests that the amount of adsorbent required may be less than the other adsorbents. Moreover, HDEHP adsorbents appear to be effective in making the separation system compact.

## Conclusions

The Sr(II) and Y(III) adsorption behaviors on the adsorbent under various conditions (different concentrations of acids ($HNO_3$ or HCl), contact times, temperatures, and concentration of metal ions) were investigated using a batch method.

The adsorption of Y(III) on the adsorbent showed high adsorptivity at low acid ($HNO_3$ and HCl) concentrations (0.001–0.5 M), but the adsorption weakened as the acid concentration was increased. On the other hand, Sr(II) was barely adsorbed. These results suggest that Y(III) can be separated from a mixed solution of Sr(II) and Y(III) using this adsorbent. Regarding the effect of the contact time, the adsorption of Y(III) on the adsorbent was well fitted to a pseudo-second-order model ($R^2 \approx 1.0$). In addition, it took several hours to reach equilibrium, but the adsorption reaction proceeded immediately after contact, and approximately half of the Y(III) in equilibrium was adsorbed within 30 min to 1 h. Regarding the effect of temperature, the results of the test showed that these adsorption processes proceeded spontaneously. The adsorption mechanism was analyzed using the Langmuir, Freundlich, and Dubinin–Raddushkevitch isotherms. The Langmuir model provided the best correlation with Y(III) adsorption on the adsorbent, indicating that the adsorption mechanism is single-layer adsorption.

The separation and recovery behavior of Y(III) from a mixed solution of Sr(II) and Y(III) using the adsorbent was tested using the column method. In the $HNO_3$ solution, separation and recovery of Y(III) were achieved, and the recovery rate was approximately 90%. On the other hand, Y(III) was eluted gradually under the HCl conditions, which was inefficient. Therefore, $HNO_3$ appears to be better than HCl.

The separation and recovery of Y(III) from a mixed solution of Sr(II) and Y(III) was achieved, and it was confirmed that this (HDEHP+Hexa)/$SiO_2$-P adsorbent has sufficient

**Table 5** Comparison with other adsorbents reported elsewhere

| Extractant | TODGA | DtBuCH18C6 | CMPO | | HDEHP | |
|---|---|---|---|---|---|---|
| Modifier | – | 1-Dodecanol | None | 1-Dodecanol | 1-Hexanol | |
| Adsorbed element | Y | Sr | Y | Y | Y | Y |
| Solution | | | | | | |
| Washing | 3.0 M $HNO_3$ | 2.0 M $NaNO_3$ and 0.1 or 0.5 M $HNO_3$ | 2.0 M $HNO_3$ | 2.0 M $HNO_3$ | 0.5 M $HNO_3$ | 0.5 M HCl |
| Elution | $H_2O$,<br>0.01 M DTPA | $H_2O$ | $H_2O$ | $H_2O$ | 3.0 M $HNO_3$ | 3.0 M HCl |
| $K_d$ of Y in washing solution (cm$^3$/g) | 120 | – | 70 | 40 | 760 | 120 |
| $k_2$ value (g/mg h) | 2.83 | – | 13 | 11 | 12.3 | 4.38 |
| $Q_e$ (mmol/g) | 4.31 | – | 0.06 | 0.42 | 0.23 | 0.24 |
| Separation behavior of Y in column | Fast | – | Fast | Fast | Fast | Slow and with tailing |
| Recovery ratio of Y(III) | 100 w% | 100% (no adsorption) | Almost 100% | Almost 100% | 89.9% | 68.7% |
| Reference | [10] | [11] | [12] | [12] | This study | This study |

capacity to separate Y(III) from a mixed solution of Sr(II) and Y(III).

## References

1. Zhamg A, Kuraoka E, Kumagai M (2007) Development of the chromatographic partitioning of cesium and strontium utilizing two macroporous silica-based calix[4]arene-crown and amide impregnated polymeric composites: PREC partitioning process. J Chromatogr A 1157:85–95
2. Wu Y, Kim SY, Tozawa D, Ito T, Tada T, Hitomi K, Kuraoka E, Yamazaki H, Ishii K (2012) Equilibrium and kinetic studies of selective adsorption and separation for strontium using DtBuCH18C6 loaded resin. J Nucl Sci Technol 49:320–327
3. Chakravarty R, Pandey U, Manolkar RB, Dash A, Venkatesh M, Pillai MRA (2008) Development of an electrochemical $^{90}$Sr-$^{90}$Y generator for separation of $^{90}$Y suitable for targeted therapy. Nucl Med Biol 35:245–253
4. Lee JS, Park UJ, Son KJ, Han HS (2009) One column operation for $^{90}$Sr/$^{90}$Y separation by using a functionalized-silica. Appl Radiat Isot 67:1332–1335
5. Innocenzi V, Michelis ID, Ferella F, Beolchini F, Kopacek B, Vegliò F (2013) Recovery of yttrium from fluorescent powder of cathode ray tube, CRT: Zn removal by sulphide precipitation. Waste Manag 33:2364–2371
6. Wang Y, Liao W, Li D (2011) A solvent extraction process with mixture of CA12 and Cyanex272 for the preparation of high purity yttrium oxide from rare earth ores. Sep Purif Technol 82:197–201
7. Tian F, Sun X, Liu X, Zhang H, Liu J, Guo H, Zhang Y, Meng C (2020) Effective adsorptive denitrogenation from model fuels over yttrium ion-exchanged Y zeolite. Chin J Chem Eng 28:414–419
8. Wanga Y, Huanga C, Li F, Donga Y, Zhaoa Z, Sun X (2016) The development of sustainable yttrium separation process from rare earth enrichments using bifunctional ionic liquid. Sep Purif Technol 162:106–113
9. Tazoe H, Obata H, Yamagata T, Karube Z, Nagai H, Yamada M (2016) Determination of strontium-90 from direct separation of yttrium-90 by solid phase extraction using DGA Resin for seawater monitoring. Talanta 152:219–227
10. Xu Y, Kim SY, Ito T, Nakazawa K, Funaki Y, Tada T, Hitomi K, Ishii K (2012) Adsorption and separation behavior of yttrium and strontium in nitric acid solution by extraction chromatography using a macroporous silica-based adsorbent. J Chromatogr A 1263:28–33
11. Kim SY, Kawamura T, Ito T (2019) Adsorption of Sr(II) and Y(III) by extraction chromatography using DtBuCH18C6-impregnated adsorbent, Global 2019, Seattle, WA, 22–27 Sept 2019
12. Kawamura T, Ito T, Kim SY (2019) Adsorption and separation behavior of strontium and yttrium using a silica-based CMPO adsorbent. J Radioanal Nucl Chem 320:9–14
13. Kudo T, Ito T, Kim SY (2017) Adsorption behavior of Sr(II) from high-level liquid waste using crown ether with ionic liquid impregnated silica adsorbent. Energy Procedia 131:189–194
14. Zhang A, Xiao C, Liu Y, Hu Q, Chen C, Kuraoka E (2009) Preparation of macroporous silica-based crown ether materials for strontium separation. J Porous Mater 17:153–161
15. Dutta S, Mohapatra PK, Raut DR, Manchanda VK (2011) Chromatographic separation of carrier free $^{90}$Y from $^{90}$Sr using a diglycolamide based resin for possible pharmaceutical applications. J Chromatogr A 1218:6483–6488
16. Tkac P, Vandegrift GF, Lumetta GJ, Gelis AV (2012) Study of the interaction between HDEHP and CMPO and its effect on the extraction of selected lanthanides. Ind Eng Chem Res 51:10433–10444
17. Ho YS, Mckay G (1999) Pseudo-second order model for sorption process. Process Biochem 34:451–465
18. Lin J, Wang L (2009) Comparison between linear and non-linear forms of pseudo-first-order and pseudo-second-order adsorption kinetic models for the removal of methylene blue by activated carbon. Front Environ Sci Eng 3(3):320–324
19. Naushad M, Al Othman ZA, Awual MR, Alam MM, Eldesoky GE (2015) Adsorption kinetics, isotherms, and thermodynamic studies for the adsorption of $Pb^{2+}$ and $Hg^{2+}$ metal ions from aqueous medium using Ti(IV) iodovanadate cation exchanger. Ionics 21:2237–2245
20. Wu H, Kim SY, Miwa M, Matsuyama S (2021) Synergistic adsorption behavior of a silica-based adsorbent toward palladium, molybdenum, and zirconium from simulated high-level liquid waste. J Hazard Mater 411:125136
21. Lima EC, Gomes AA, Tran HN (2020) Comparison of the nonlinear and linear forms of the van't Hoff equation for calculation of adsorption thermodynamic parameters (ΔS° and ΔH°). J Mol Liq 311:113315

22. Ghaemi A, Torab-Mostaedi M, Ghannadi-Maragheh M (2011) Characterizations of strontium(II) and barium(II) adsorption from aqueous solutions using dolomite powder. J Hazard Mater 190:916–921
23. Ueberbacher R, Rodler A, Hahn R, Jungbauer A (2010) Hydrophobic interaction chromatography of proteins: thermodynamic analysis of conformational changes. J Chromatogr A 1217:184–219
24. Foo KY, Hameed BH (2010) Insights into the modeling of adsorption isotherm systems. Chem Eng J 156:2–10
25. Al-Ghouti MA, Da'ana DA (2020) Guidelines for the use and interpretation of adsorption isotherm models: a review. J Hazard Mater 393:122383
26. Dada AO, Olalekan AP, Olatunya AM, Dada O (2012) Langmuir, Freundlich, Temkin and Dubinin–Radushkevich isotherms studies of equilibrium sorption of $Zn^{2+}$ unto phosphoric acid modified rice husk. J Appl Chem 3(1):28–45
27. Zhang A, Hu Q (2010) Adsorption of cesium and some typical coexistent elements onto a modified macroporous silica-based supramolecular recognition material. Chem Eng J 159:58–66